AAS 06-190

THE ROLE OF INVARIANT MANIFOLDS IN LOW THRUST TRAJECTORY DESIGN (PART III)

Martin W. Lo,[*] Rodney L. Anderson,[†] Try Lam,[*] and Greg Whiffen[*]

This paper is the third in a series to explore the role of invariant manifolds in the design of low thrust trajectories. In previous papers, we analyzed an impulsive thrust resonant gravity assist flyby trajectory to capture into Europa orbit using the invariant manifolds of unstable resonant periodic orbits and libration orbits. The energy savings provided by the gravity assist may be interpreted dynamically as the result of a finite number of intersecting invariant manifolds. In this paper we demonstrate that the same dynamics is at work for low thrust trajectories with resonant flybys and low energy capture. However, in this case, the flybys and capture are effected by continuous families of intersecting invariant manifolds.

INTRODUCTION

This paper is the third and last in a series to explore the role of invariant manifolds in the design of low thrust trajectories. Our stated goals were to first, demonstrate that invariant manifolds do indeed play a role in low thrust trajectories, and second, explain how the dynamics of low thrust interplanetary trajectories interact with invariant manifolds (see Lo and Anderson[1]). In the first paper (just cited), we compared low thrust trajectories to invariant manifolds of nearby unstable orbits at a single energy level. This suggests heuristically that we are on the right track, but since low thrust trajectories are constantly changing their Jacobi energy while thrusting, one must study the entire family of invariant manifolds in the energy range of the low thrust trajectory. In order to do this, we must first understand the role of resonant orbits in planetary flybys, whether invariant manifolds play a role or not. Thus, in the second paper (Anderson and Lo[2]), we analyzed the Planar Europa Orbiter (PEO) trajectory and found that it indeed follows the stable and unstable manifolds of the resonant orbits between impulsive maneuvers. In particular, where the manifolds intersect in configuration space but not in phase space, those are the locations where a maneuver is required for moving from one manifold to another. This suggests that a deeper understanding of the geometry of the invariant manifolds of resonant orbits is critical to

[*]Jet Propulsion Laboratory, California Institute of Technology, Pasadena, CA 91109
[†]The Colorado Center for Astrodynamics Research, University of Colorado, Boulder, CO 80309

understanding planetary flybys, and we anticipate, for low thrust trajectories as well when they are moving through resonant orbit regions. In this paper, we examine the relations between a low thrust trajectory and the invariant manifolds of several families of resonant orbits through the energy levels traversed by the low thrust trajectory. A more detailed version of the results summarized in this paper may be found in Anderson's dissertation[3].

The use of low thrust in trajectory design can significantly increase the complexity of the design process, since many of the standard astrodynamics tools are no longer applicable without what are sometimes significant modifications. For modeling performed in the two-body problem, it increases the difficulty of design in that the resulting trajectory no longer follows conic sections. In the three-body problem, the energy or the Jacobi constant changes as a result of the constant thrust. As a result of these difficulties, much of the design work for low thrust missions is performed using optimization tools which do not necessarily incorporate full knowledge of the dynamics of the problem from a dynamical systems perspective in the search for a desired trajectory. It has been observed however, that the solutions developed using the Mystic optimization software appear to generally follow the same types of paths as the invariant manifolds of unstable periodic orbits in the three-body problem[4]. The question then arises as to whether a knowledge of the relationship of these optimized trajectories to the invariant manifolds of unstable orbits could prove useful in the design of these trajectories. The long periods of time required to run the optimization software could be significantly reduced if an initial guess could be developed using the dynamics of the problem in the form of the invariant manifolds of the relevant unstable orbits.

MODELS AND TOOLS

The Circular Restricted Three-Body Problem

The Circular Restricted Three-Body Problem (CRTBP) was the primary model used in this study. Many references exist with overviews from previous works[2, 3] or more detailed explanations[5, 6] of this problem, but it is briefly described here. In this model, a large body (the primary) and a smaller body (the secondary) are assumed to rotate about their center of mass in circular orbits*. The objective is to describe the motion of a third infinitesimal mass, typically representing a spacecraft, placed in this system. In order to simplify the analysis for this study, the infinitesimal mass was further restricted to the plane of motion of the two primaries. The resulting problem is then commonly referred to as the planar or coplanar CRTBP (PCRTBP). An integral of motion also exists in this model called the Jacobi Constant, which varies when maneuvers are performed. Finally, there are five equilibrium points in the problem about which periodic libration point orbits exist.

*The value of μ used for the Jupiter-Europa system in this study was approximately $\mu = 2.526645 \times 10^{-5}$, where μ is defined as the dimensionless mass of the secondary and $1 - \mu$ as the dimensionless mass of the primary.

Poincaré Maps

Once again, this tool has been described in earlier works[2, 3], but as it is essential to this analysis, it will be briefly reviewed here. In order to compute a Poincaré map for a system in $\mathbb{R}^n$, a 'hypersurface' Σ or surface of section in $\mathbb{R}^{n-1}$ is placed tranverse to the flow as shown in Figure 1. A trajectory intersecting the surface of section is integrated until

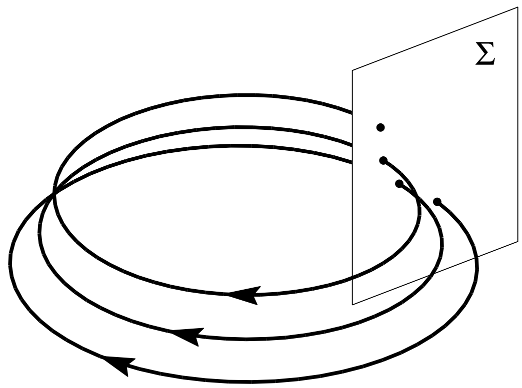

Figure 1 Sample Poincaré map for a three-dimensional system

it intersects the surface of section once again. The mapping is from the first intersection to the next intersection and so on. The points of the mapping may then be plotted using a number of different coordinates. These Poincaré surface of sections or Poincaré sections allow the location of stable periodic and quasi-periodic orbits to be computed. For the PCRTBP in $\mathbb{R}^4$, the surface of section is specified by fixing one of the coordinates in order to produce a surface in $\mathbb{R}^3$. In this analysis, the surface of section is specified by $y = 0$ along the x-axis opposite Europa (see Figure 4).

PLANAR GANYMEDE TO EUROPA TRAJECTORY

This analysis focuses on a nearly planar low thrust trajectory developed by Lam[7] using Mystic which travels from near Ganymede to Europa in the Jupiter-Europa CRTBP. This trajectory is shown in both the inertial and rotating frames in Figure 2. As mentioned previously, the convergence process in Mystic did not allow the trajectory to remain completely planar, but the maximum deviation from the plane was only 7.4 km or 1.1×10^{-5} dimensionless distance units. This was judged to be sufficiently planar that the previously developed techniques should still be adequate for this analysis. Examining the trajectory in the inertial frame indicates the possible presence of three distinct periods or resonances. The variation in the number of loops on the trajectory in the rotating frame also confirms that the trajectory is traveling through at least two resonances. This is not as clear as in the case of the impulsive planar Europa Orbiter (PEO) trajectory analyzed previously[1, 2], as the energy is changing at many points on the trajectory rather than just at two points. Finally, the trajectory as it approaches Europa appears to possess the characteristics of a Distant Retrograde Orbit (DRO).

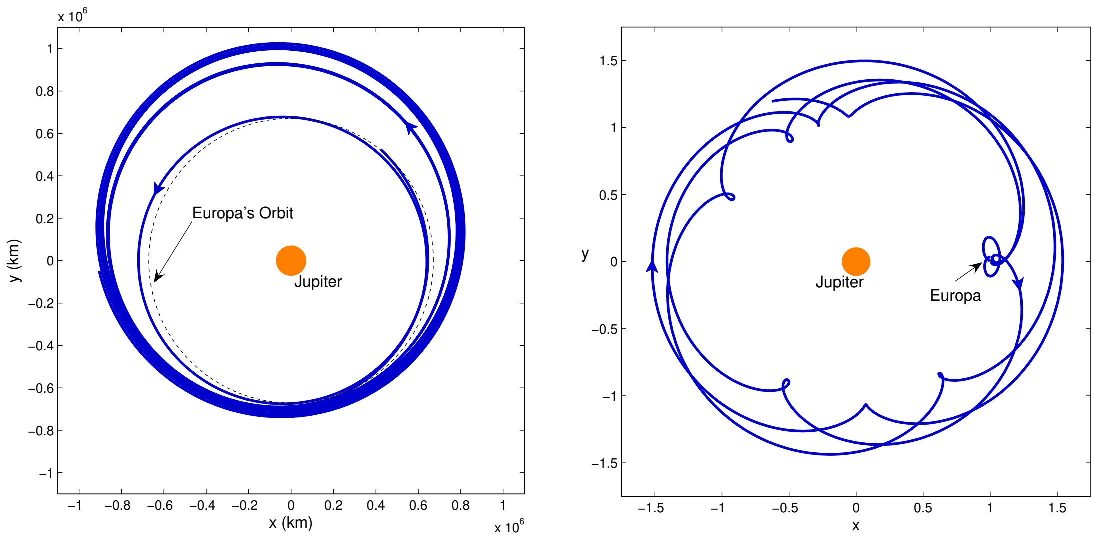

(a) Inertial Frame (b) Jupiter-Europa Rotating Frame

Figure 2 The planar low thrust trajectory traveling from near Ganymede to Europa.

The effect of low thrust on the characteristics of the trajectory may be quantified using both two-body and three-body parameters. The thrust profile over the trajectory shown in Figure 3(a) indicates the presence of multiple extended periods of thrusting. Even during the regions that appear to be gaps, thrusting on the order of 1.0 mN takes place. Examining the Jacobi constant in Figure 3(b) confirms the expectation that the Jacobi constant undergoes its major changes during periods of higher thrusting. The slight changes observed in the other regions are due to the fact that some small thrust is still being applied. At first it seems curious that, unlike the PEO, this trajectory is traveling from a higher Jacobi constant to a lower Jacobi constant. However, it should be noted that the low thrust trajectory is traveling from Ganymede which would generally have a high Jacobi constant of approximately 3.15 if it were computed in the Jupiter-Europa system. The PEO is attempting to approach Europa from a more energetic trajectory which would correspond to a lower Jacobi constant. The two-body period in Figure 3(c) appears to undergo some changes as a result of the thrusting, but the variations elsewhere along the trajectory arise from the three-body perturbations. These results are consistent with those of the PEO which saw changes in the period between ΔVs as a result of flybys.

Previously analyzed trajectories[3] have a demonstrated relationship with the invariant manifolds of unstable periodic orbits, so it is expected that the low thrust trajectory may possess a similar connection. Determining whether such a relationship exists requires the computation of the invariant manifolds of the correct unstable periodic orbits at each energy level found on the low thrust trajectory. The relevant unstable orbits may be unknown initially, but at least for resonant orbits, a guess as to the appropriate resonance may be obtained by using the two-body periods calculated along the trajectory. The technique developed in previous papers of using Poincaré sections to visualize the relationship of the trajectory to the invariant manifolds is used here with a Poincaré section including the relevant dynamical structures.

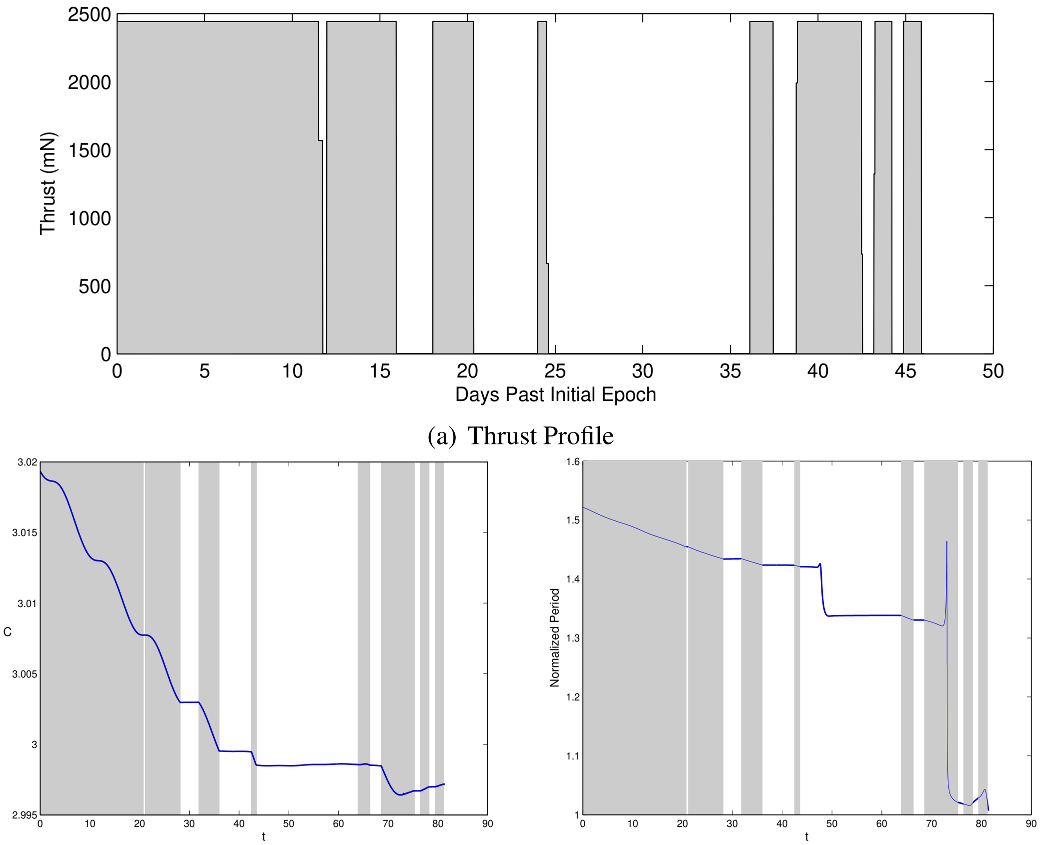

(a) Thrust Profile

(b) Jacobi Constant

(c) Period Normalized by Europa's Period

Figure 3 Changes in three-body and two-body parameters compared to the thrust profile. Gray shading indicates periods of significant thrust. The two-body period was computed with respect to the barycenter. The dimensionless time is indicated by t.

First, however, the intersections with the surface of section[†] of the instantaneous state on the low thrust trajectory integrated forward and backward in time were computed. In this process, the state at each point on the low thrust trajectory was first selected neglecting the z components. This state was then integrated backward in time without thrust until it intersected the surface of section, and this point was recorded. Next, the same state was integrated forward in time without thrust until it intersected the surface of section. This is illustrated for a single point on the low thrust trajectory in Figure 4. This process allows a comparison of these points with the invariant manifolds at the surface of section rather than attempting the rather more difficult proposition of comparing the trajectories to the invariant manifolds in phase space. Examining these intersections by themselves in Figure 5 reveals structures that appear to be somewhat similar to the invariant manifolds computed for the PEO trajectory. This indicates the existence of a possible relationship to the invariant manifolds, but a more thorough analysis including the various dynamical structures at each energy level must be performed.

[†]Note that the surface of section used throughout this paper is at the same location as shown in Figure 4.

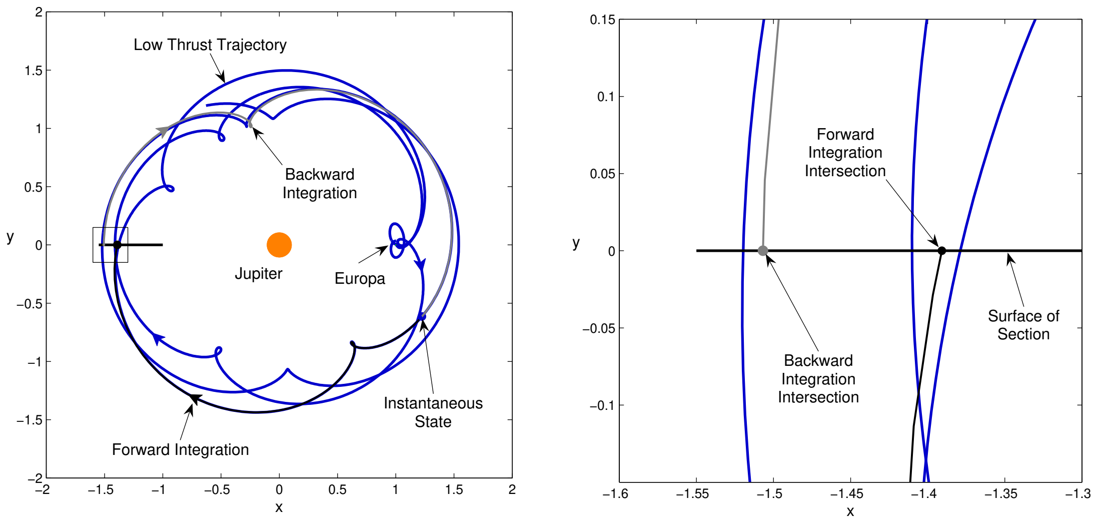

(a) Trajectory Overview (b) Boxed Region

Figure 4 Illustration of the computation of the points in the Poincaré section for the low thrust trajectory. The points integrated without thrust intersect the surface of section at different points from the low thrust trajectory.

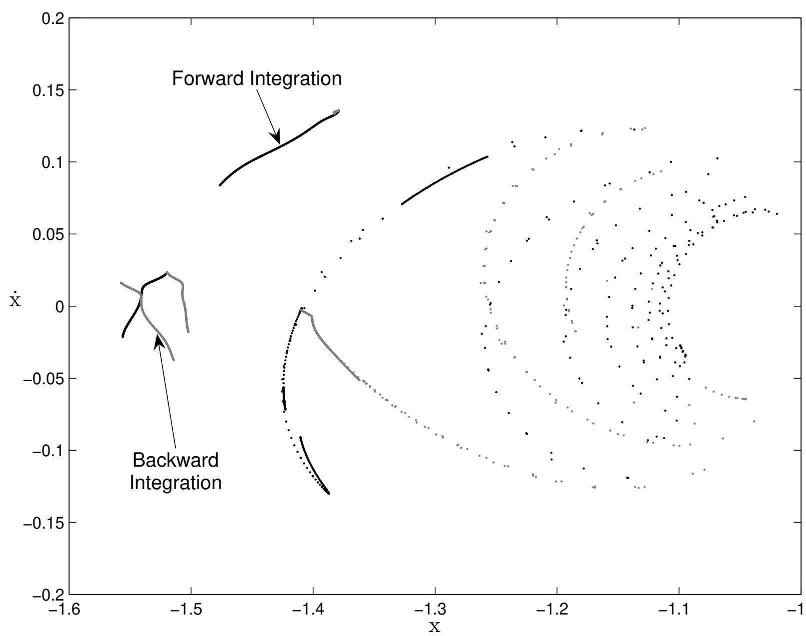

Figure 5 Intersections with the surface of section of individual points on the low thrust trajectory integrated forward and backward in time. The instantaneous state at each point on the trajectory was used in the integration, which did not include any thrust.

RESONANT ORBITS

The primary dynamical structures of interest in this analysis are resonant orbits and their invariant manifolds. The low thrust trajectory appears to travel between different resonances, so it is natural to expect the existence of a relationship between this trajectory and the three-body resonant orbits at these resonances. More specifically the relationship to the resonant orbits possessing the same Jacobi constant is of interest. An initial guess for a resonant orbit at a desired resonance may be obtained using the integration of large numbers of orbits and Poincaré sections. Once this initial guess has been obtained, it may be converged to a truly periodic orbit symmetric about the x-axis using standard single shooting techniques[8]. After the initial resonant orbit has been found, the problem is then to continue the orbit to obtain a resonant orbit at the desired energy. Although a wide variety of continuation techniques have been developed, a simple linear extrapolation of conditions along the x-axis was found to be sufficient for this study of resonant orbits. Once a series of orbits across a range of Jacobi energies have been found, a simple secant method can be used to compute a resonant orbit at any desired energy value.

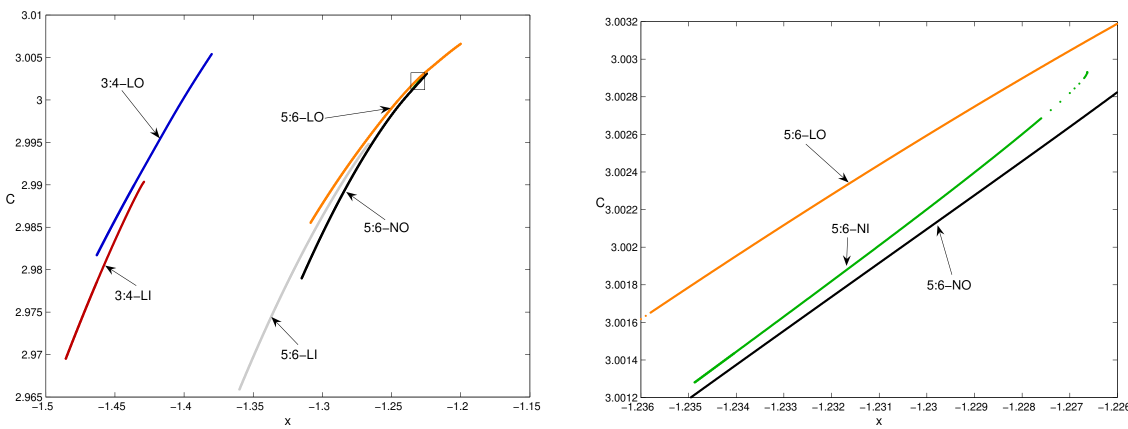

(a) Continuation Plot Overview (b) Boxed Region

Figure 6 Continuation plot for the 3:4 and 5:6 resonant orbits. The points represent the initial conditions on the x-axis for each of the converged orbits. Each family is labeled first by the resonance. They are then labeled according to whether they pass through the inner (I) region between Jupiter and Europa or the outer (O) region. Finally, they are also labeled according to whether a loop exists on the line of syzygy (L) or not (N).

The continuation plots in Figure 6 give a summary of the families of orbits found at the 3:4 and 5:6 resonances using the current techniques. Although not necessarily expected, it appears that several different types of unstable resonant orbits may exist at each resonance for a given energy level. In each case the family was continued until the linear extrapolation method failed to converge on a trajectory in the same family. In these cases, the points on the continuation plot typically took an abrupt turn as can be seen in Figure 6(b) where the 5:6-NI family turns, and the family can no longer be continued using this method. This might be a sign of a bifurcation, but additional techniques would be required to analyze this phenomena.

A selection of the converged orbits in the 3:4-LO and 5:6-LO families are shown in Figures 7 and 8 at even intervals of energy. These families were found to be of the most interest for the given low thrust trajectory. It can also be noted that the limit in the continuation is often either the point where the family encounters Europa or where a change in the topology of the trajectory occurs. For a more detailed analysis of all of these families see Anderson[3].

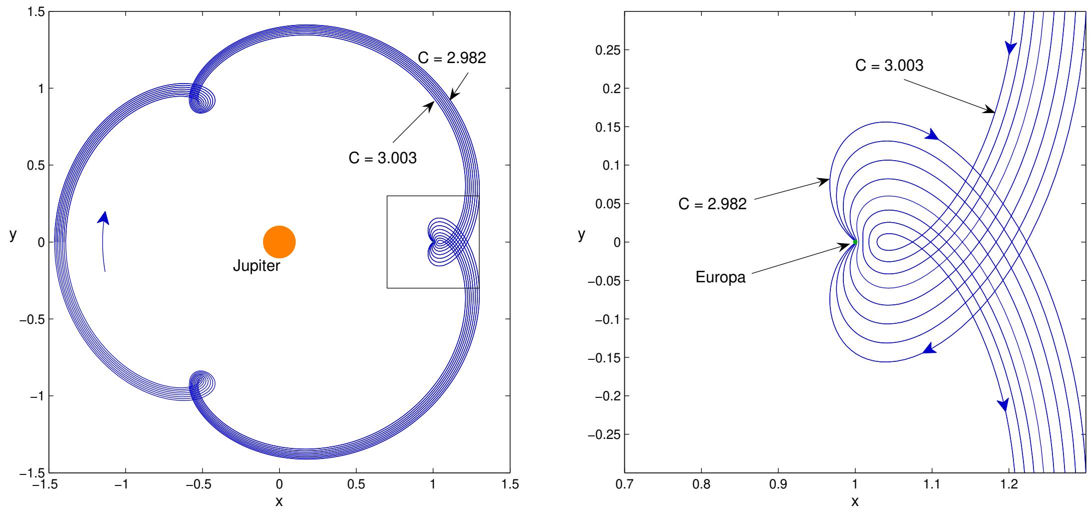

(a) Resonant Orbit Family Overview

(b) Boxed Region

Figure 7 Orbits in the 3:4-LO family. The Jacobi constant of the two bounding trajectories are labeled, and the intermediate trajectories vary linearly in their Jacobi constant in increments of 0.003.

COMPARISON WITH INVARIANT MANIFOLDS

Ideally, a study of the relationship of the low thrust trajectory to the invariant manifolds of unstable orbits would include a comparison in phase space of each instantaneous point on the trajectory with the invariant manifolds computed at the energy of that point. As mentioned previously, this approach quickly becomes cumbersome even in configuration space, making the use of Poincaré sections desirable. These Poincaré sections were computed for each of the desired points on the trajectory in order to understand how the low thrust trajectory moved relative to the invariant manifolds as thrust was applied. The initial portion of the low thrust trajectory contained points at Jacobi constants above the range computed for the unstable resonant orbit families. Therefore, this analysis starts approximately 14.3 days after the initial epoch on the low thrust trajectory. The Poincaré sections computed for each point on the low thrust trajectory were generally viewed as a movie of which some of the frames are discussed next.

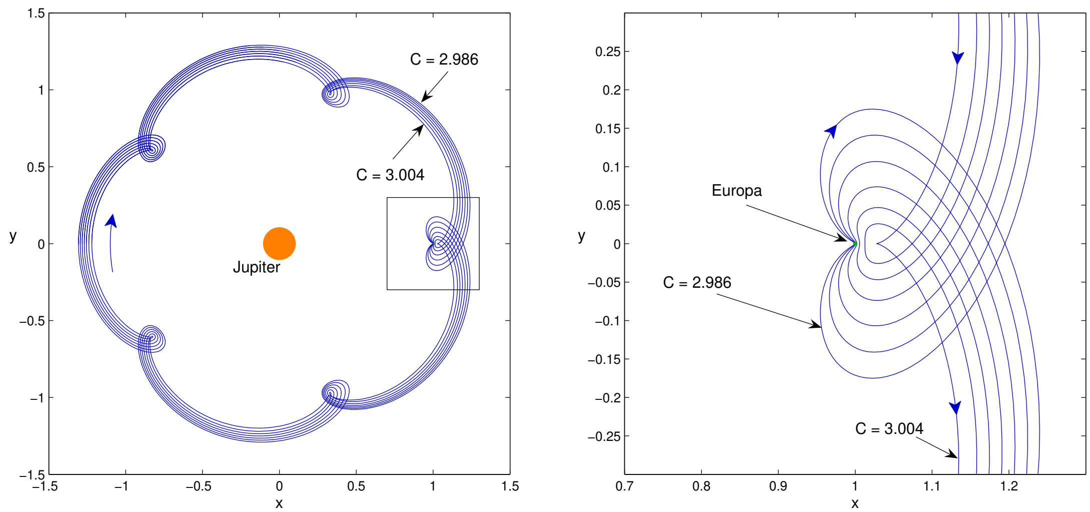

(a) Resonant Orbit Family Overview

(b) Boxed Region

Figure 8 Orbits in the 5:6-LO family. The Jacobi constant of the two bounding trajectories are labeled, and the intermediate trajectories vary linearly in their Jacobi constant in increments of 0.003.

The first frame shown in Figure 9 starts off at the highest Jacobi constant in this analysis‡. The same convention introduced earlier holds here where a black point represents a state on the low thrust trajectory integrated forward, while a gray point represents a backward integration. Now, however, only the two points corresponding to the energy level of the specified Poincaré section are plotted. In this first frame, the point obtained from the backward integration is not visible as it is to the left of the plot, but the forward integration gives a point somewhat distant from the invariant manifolds. It is suspected that it might lie close to the invariant manifold of another unstable resonant orbit that was simply not computed for this study. As time progresses though, the stable invariant manifold of the 3:4 resonant orbit appears to approach the forward integration intersection as it also moves slightly. In Figure 9(e) as the point integrated backward comes closer to the stable manifold of the 3:4 resonant orbit, the forward integrated point is found to lie nearer the 3:4 resonant orbit close to its unstable manifold. This observation makes sense as it would be expected that points close to the stable manifold of an unstable orbit would come closer to that orbit over time. The relationship with the stable manifold is even more clearly seen in Figure 9(f) where the thrust has modified the trajectory so that the backward integration appears to lie on the stable manifold of the 3:4 orbit. The next intersection then lies nearly on top of the 3:4 orbit, just as the stable manifold would behave. Overall it is also interesting to observe the changes in the invariant manifolds of the resonant orbits over the range of Jacobi constants in the frames in Figure 9. The invariant manifolds move from having relatively few intersections with themselves to possessing the large number of intersections at many resonances seen in Figure 9(f). The optimization algorithm appears to be using low thrust

‡Note that the same color convention used in Figure 9(b) applies to all of the Poincaré sections. The labels are typically not shown so that the manifolds are not obscured.

both to move the intersection of the trajectory around the Poincaré section as well as to move to different energies where the invariant manifolds are located in positions that may be used by the trajectory.

In Figure 10, the series of plots begins with the backward integrated point located near the previous location of the forward integrated point. This switch often occurs when the trajectory passes through the surface of section. The forward integrated point now lies nearly on the unstable manifold of the 3:4 orbit. This makes sense as the backward integrated point actually lies just off the 3:4 orbit on its unstable manifold, and the next intersection is naturally further away from the 3:4 orbit on the unstable manifold. As time continues, the thrust is used to move the backward integrated point slightly toward the stable manifold of the 5:6 orbit. As this is done, the forward integrated point moves backward along the unstable manifold of the 3:4 orbit in the Poincaré section. It then continues to generally follow the unstable manifold of the 3:4 orbit which lies very near the unstable manifold of the 5:6 orbit. Remember that it is the optimization algorithm that has selected this path for the trajectory, and it is very interesting that nearly all the points in the sequence lie very near the unstable manifold. It indicates that the optimization algorithm has converged on the invariant manifolds as optimum pathways between resonances. The relationship of the low thrust trajectory to the invariant manifolds over time can be even more clearly seen by plotting each of the intersections of the low thrust trajectory over the time range covered by Figure 10 as was done in Figure 11. Here, although the energy is changing over this time range, the difference in the invariant manifolds is small enough that the way in which the low thrust intersections follow the invariant manifolds may still be observed.

The frames in Figure 12 continue the sequence starting at the next major thrusting period. The first five frames at the beginning of this thrusting period reveal significant changes in the location of the forward integrated point as it appears to move from the 3:4 resonance in the previous sequence of plots to the 5:6 resonance along the unstable manifolds of the 3:4 and 5:6 orbits. Through this process, the backward integrated point moves slightly along the stable manifold of the 5:6 orbit as it begins to approach the 5:6 orbit. As before, it is not unexpected that the fact that the backward integrated point lies near the stable manifold of the 5:6 orbit would produce a forward integrated point that is then closer to the general vicinity of the 5:6 orbit. The fact that the forward integrated point lies near the unstable manifolds of both the resonant orbits is curious. Integrating the point on the stable manifold of the 5:6 orbit closest to the backward integrated point shows that the next intersection of the stable manifold is nearly on top of the 5:6 orbit. So the slight difference in initial conditions between the stable manifold of the 5:6 orbit and the backward integrated point result in a large difference in the location of the next intersection. Overall, this sequence of plots aids in revealing the method by which the optimization scheme has used low thrust to perform a resonance transition. In Figure 12(f), the backward integrated point continues to move along the stable manifold of the 5:6 orbit, and the forward integrated point moves past the 5:6 resonance. Beyond this time period, the trajectory begins the approach phase at Europa using a DRO. Further analysis at this point requires the selection of a new surface of section, since the current surface of section is on the opposite side of Jupiter from the DRO.

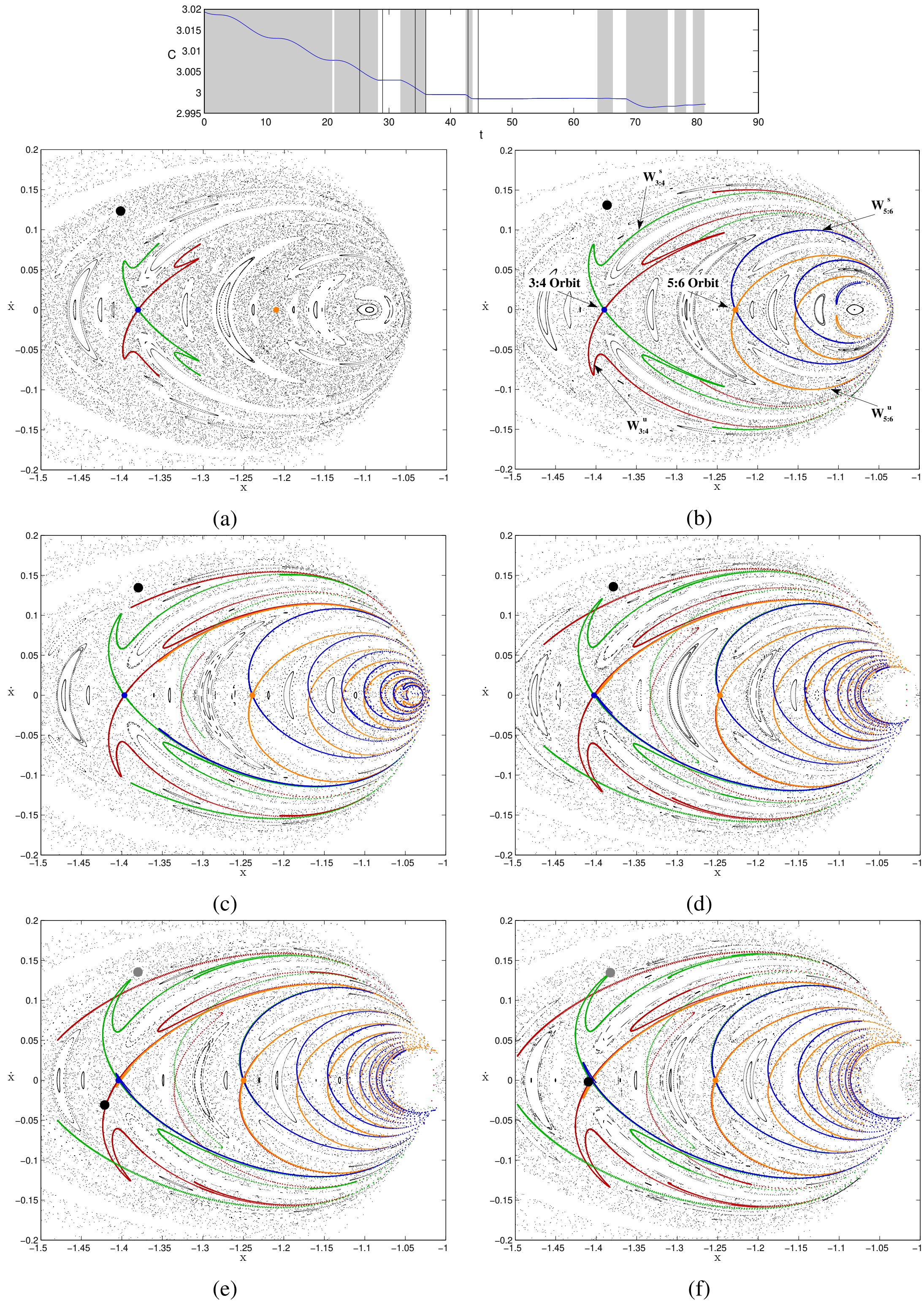

Figure 9 Poincaré sections (a−f) for various points on the low thrust trajectory. The vertical lines on the Jacobi constant plot (top) indicate the times corresponding to each Poincaré section which are plotted sequentially.

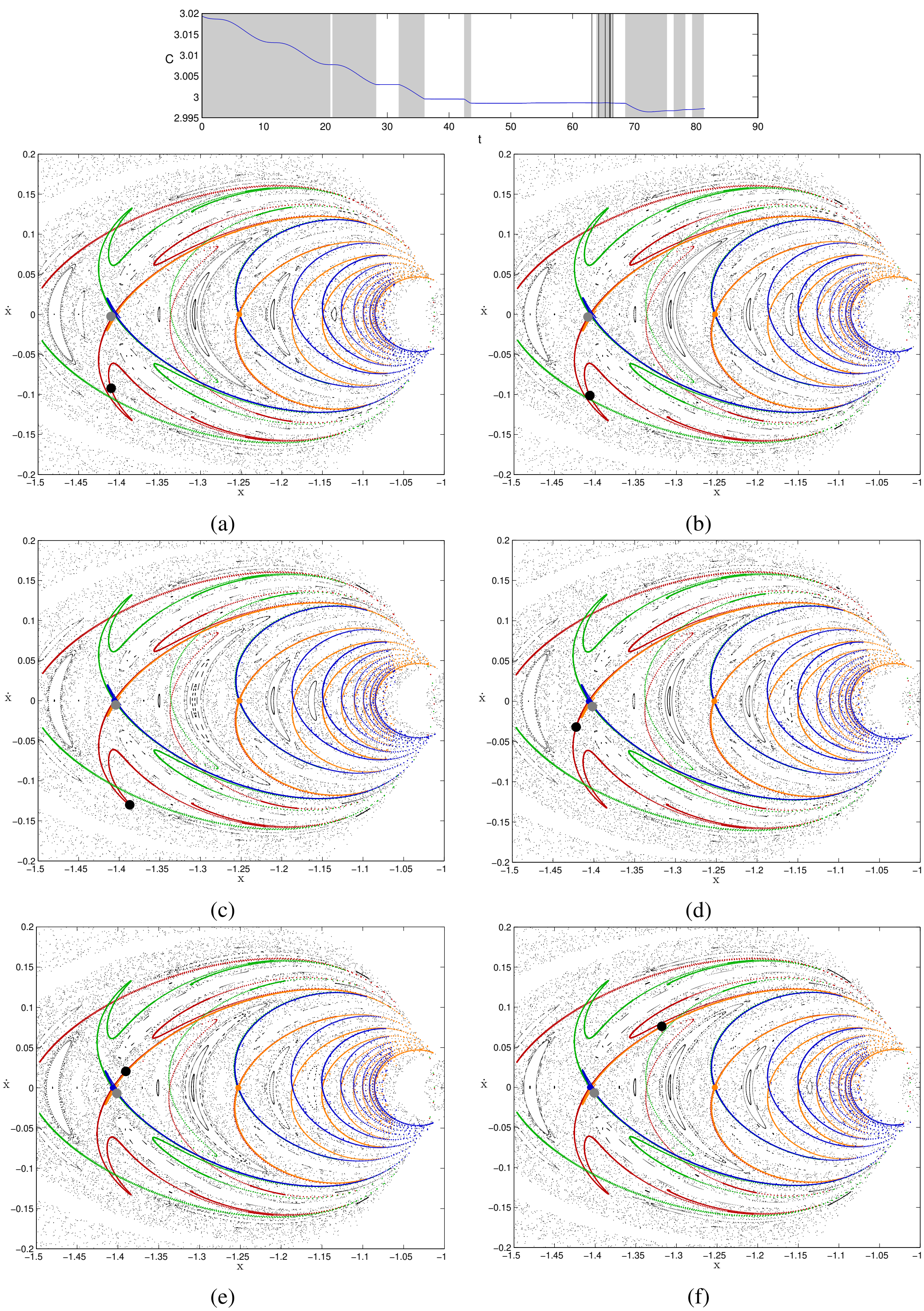

Figure 10 Poincaré sections (a−f) for various points on the low thrust trajectory. The vertical lines on the Jacobi constant plot (top) indicate the times corresponding to each Poincaré section which are plotted sequentially.

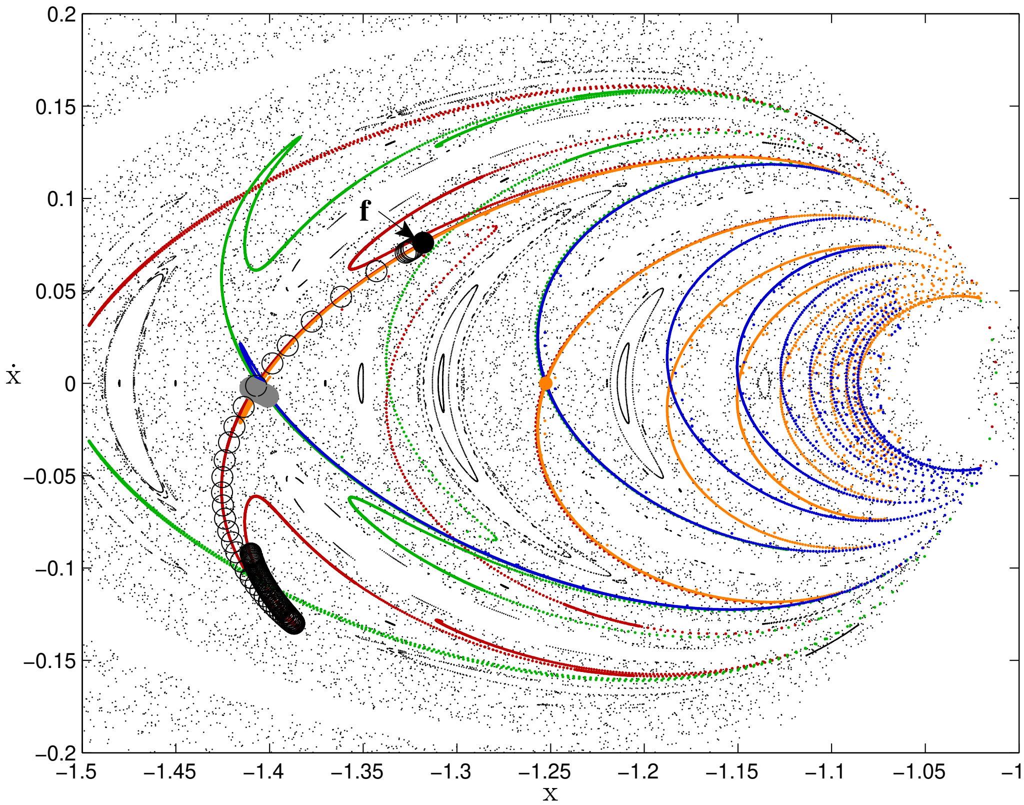

Figure 11 Summary plot showing the intermediate low thrust trajectory intersections leading from Figure 10(a) to Figure 10(f). The background points and the invariant manifolds are plotted at the energy level of Figure 10(f), and the empty circles indicate intersections computed at a different energy levels. The initial points appear black because there are so many of them, but the only point at the current energy level is the point labeled f.

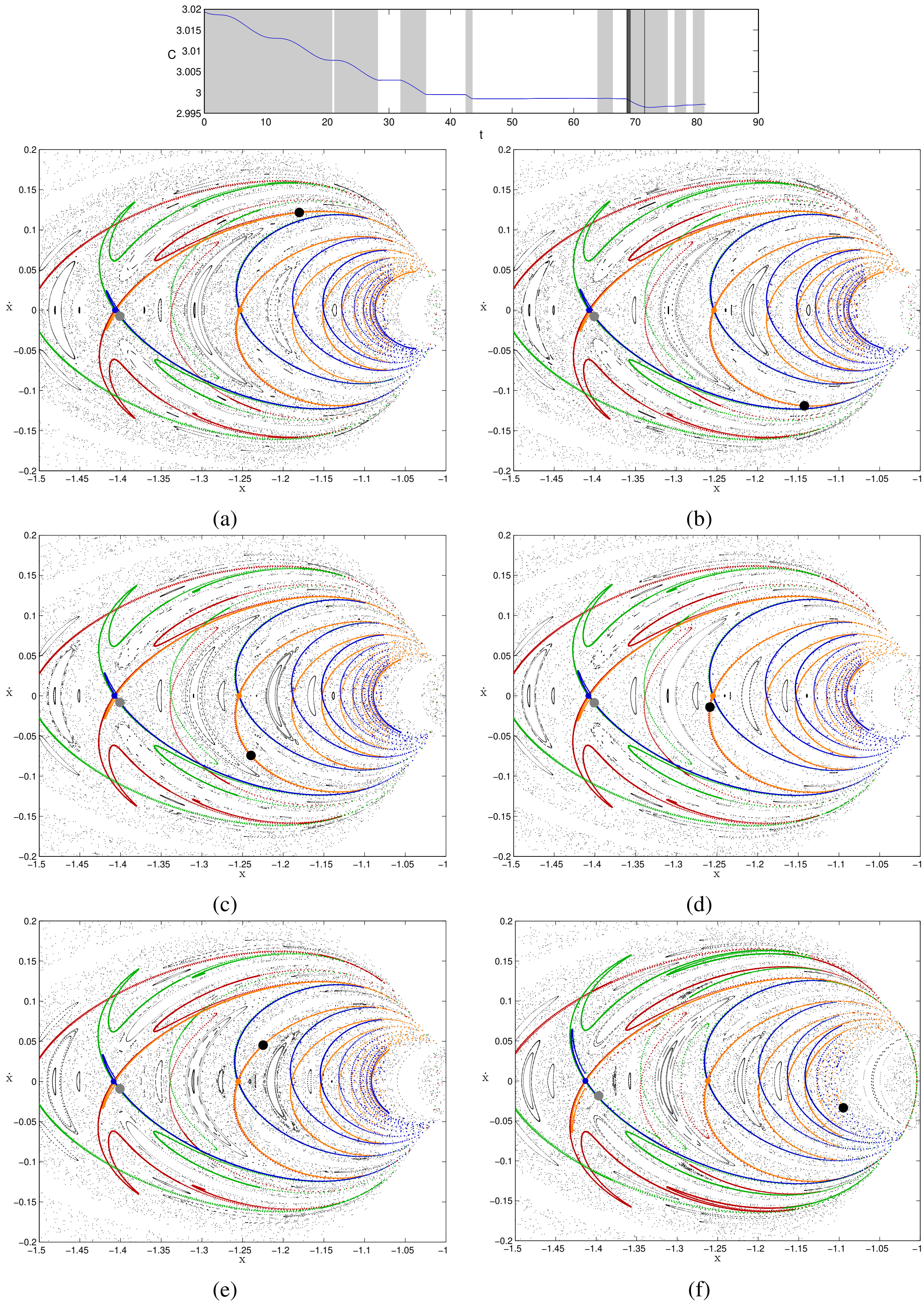

(a) (b)

(c) (d)

(e) (f)

Figure 12 Poincaré sections (a−f) for various points on the low thrust trajectory. The vertical lines on the Jacobi constant plot (top) indicate the times corresponding to each Poincaré section which are plotted sequentially.

CONCLUSION

The fact that most of the intersections of the low thrust trajectory lie very near the stable or unstable manifolds of one of the resonant orbits indicates that the optimization algorithm is converging on trajectories that generally follow the invariant manifolds. This result is especially interesting since the optimization algorithm does not incorporate any knowledge of the invariant manifolds in its search for a trajectory. Knowledge of this relationship has the potential to be very useful in developing initial guesses for these optimization algorithms, and ultimately it should aid in developing control laws for new optimization algorithms that could find pathways for low thrust trajectories using invariant manifolds.

In these three papers, we have demonstrated that invariant manifolds do indeed play a significant role in the dynamics of low thrust trajectories moving through unstable regions. Resonant orbits, which play such an important role for impulsive planetary flybys, also play an important role for low thrust trajectories. In fact, we have shown that planetary flybys are also dynamically controlled by invariant manifolds of unstable resonant orbits, despite the fact that they are typically designed using patched conic methods with great success.

Finally, in this last paper, we have demonstrated that kinematically low thrust trajectories closely track the invariant manifolds of the unstable resonant orbits. From this observation there are several near-term projects that should be investigated.

FUTURE WORK

We have but scratched the surface in our investigation of the dynamical role of invariant manifolds in the control and optimization of low thrust trajectories. Nevertheless, it would be exciting to develop some rough algorithms to produce initial guess trajectories as inputs for optimization programs such as Mystic and compare the time savings from more conventional initial guess solutions.

Another longer term and more academic project is the investigation of the topology and geometry of invariant manifolds of unstable resonant orbits and their role in the optimization of low thrust trajectories. In our second paper (Anderson and Lo[2]), the intersection geometry of the invariant manifolds of resonant orbits dictated the need for maneuvers. It would be interesting to investigate how the thrust profile of the low thrust trajectory compares with the intersection geometry of the manifolds. Another interesting problem, perhaps less profound, but who can say for sure, is the manner in which the low thrust trajectory is cutting through the invariant manifolds. For example, what is the angle of the thrust vector to the invariant manifold surface (in the planar RTBP)? What does the control of this angle do? How does this angular profile compare with the gradient across the surfaces of the invariant manifold? With the recent advances in computational differential geometry and algebraic topology, it would seem that many advanced tools are just waiting for us, engineers, to make use of them.

Although we have only examined the role of invariant manifolds in low thrust trajectories going through unstable regions, they also play a similar role in stable regions. In fact, a surprising thing at first is the observation that low thrust trajectories through unstable regions are easier to design (using a tool like Mystic) than the spiral trajectories in the two-body problem. Here is a rich problem indeed that needs to be examined using more advanced mathematical methods. While stable and unstable manifolds do not play a role here, the invariant tori of stable elliptical trajectories do indeed play a role. A similar type of analysis can and should be performed for such trajectories to obtain better approximations.

Lastly, the understanding that invariant manifolds play a central role in impulsive planetary flyby trajectories is very exciting indeed. Perhaps this is not so surprising since Tisserand's Criteria for comets is just the linearization of the Jacobi constant. This means that we can reconceptualize planetary flyby trajectories using invariant manifold theory just as we have been doing for libration orbits and low energy orbits in general. The distinction between high and low energy orbits is perhaps not as distinct as we have once thought. The implication of this observation is that one can conceive of a unified theory to describe both low energy and high energy trajectories, and both impulsive and low thrust trajectories. This unification, while interesting and beautiful in itself, has far reaching consequences for the future of astrodynamics and mission design.

For instance, because invariant manifolds can be predicted and precomputed as maps on board spacecraft, it is conceivable that autonomous on-board trajectory design and optimization as well as mission design and planning may be achieved in the near future. These maps do not need to be full blown ephemerides, one need only a network of initial conditions perhaps even using a simple model like the CRTBP. By continuation methods and interpolation, full ephemeris model trajectories may be generated on board future spacecraft to perform the mission design and optimization. But even before going on-board spacecraft, such a technology will greatly speed up our ability to design, analyze, and optimize complex missions in multi-dynamical regimes and with any combination of propulsion systems.

Clearly, there is a lot of work ahead of us. Perhaps with these ideas we can approach funding agencies, policy makers, and university departments to obtain support for research and technology development. Astrodynamics is by no means a done deal, despite our many successes in the last century. We are on the verge of a new intellectual revolution in astrodynamics that will help us explore and develop the Solar System in ways that were beyond our reach in the last century.

ACKNOWLEDGMENTS

The authors would like to thank Dr. George Born for his continuing support of this research. They would also like to thank Dr. Bob Easton for many helpful discussions. This work was conducted at the Jet Propulsion Laboratory, California Institute of Technology, under contract with the National Aeronautics and Space Administration. It was specifically supported by the Prometheus project. The supercomputer used in this investigation was provided by funding from JPL Institutional Computing and Information Services and the NASA Offices of Earth Science, Aeronautics, and Space Science.

REFERENCES

1. Lo, M. W., Anderson, R. L., Whiffen, G., and Romans, L., "The Role of Invariant Manifolds in Low Thrust Trajectory Design (Part I)," Paper AAS 04-288, AAS/AIAA Spaceflight Dynamics Conference, Maui, Hawaii, February 8-12, 2004.

2. Anderson, R. L. and Lo, M. W., "The Role of Invariant Manifolds in Low Thrust Trajectory Design (Part II)," 2004, Paper AIAA 2004-5305, AIAA/AAS Astrodynamics Specialist Conference, Providence, Rhode Island, August 16-19.

3. Anderson, R. L., *Low Thrust Trajectory Design for Resonant Flybys and Captures Using Invariant Manifolds*, Ph.D. Thesis, University of Colorado at Boulder, 2005.

4. Lo, M. W., "The Interplanetary Superhighway and the Origins Program," 2001, IEEE.

5. Roy, A. E., *Orbital Motion*, Adam Hilger, Philadelphia, Pennsylvania, 3rd ed., 1988.

6. Szebehely, V., *Theory of Orbits: The Restricted Problem of Three Bodies*, Academic Press, New York, 1967.

7. Lam, T., "Ganymede to Europa in Mystic's Circular Restricted Three Body Model," Interoffice memo, Jet Propulsion Laboratory, October 2004.

8. Howell, K. C. and Breakwell, J. V., "Three-Dimensional, Periodic, 'Halo' Orbits," *Celestial Mechanics*, Vol. 32, 1984.